On the Conformation of Phenylalanine Specific Transfer RNA

Studies on Size and Shape of the Molecule by X-Ray Small Angle Scattering

Ingrid PILZ and Otto KRATKY

Institut für Physikalische Chemie der Universität, Graz

Friedrich CRAMER, Friedrich von der HAAR, and Eckhard SCHLIMME

Max-Planck-Institut für Experimentelle Medizin, Abteilung Chemie, Göttingen

(Received December 5, 1969/March 31, 1970)

The scattered X-ray intensities from dilute solutions of $tRNA^{Phe}$ (yeast) in 0.05 M Tris buffer at pH 7.5 were measured at 17°. The radius of gyration R (24.4 Å), the molecular weight M (26100) and the volume V (41500 Å^3) were determined.

A comparison of experimental with theoretical scattering curves of different bodies shows that the shape of the molecule cannot be well represented by a simple triaxial body. The calculated scattering curves which fit the measured scattering data best are for an elongated body with two different cross-sections.

No significant change of X-ray small angle scattering was observed on increasing the temperature from 17° to 40°. At higher temperatures the radius of gyration is increased with increasing temperature and at 70° the molecule has a random coil conformation.

To get more detailed information about the process of activation of amino acids during protein synthesis by the tRNA-aminoacyl synthetase system a detailed knowledge of the structure of tRNA is necessary. Although several sequences (= primary structures) of tRNAs are known, one cannot derive secondary and tertiary structures from these sequences. In this respect the situation is similar to that in the protein field.

The method of X-ray small angle scattering yields information on shape and dimensions of macromolecules in solution [1]. Previously a mixture of tRNAs [2] as well as purified $tRNA^{Ala}$ (yeast) [3] and $tRNA^{Val\,I}$ (*E. coli*) [4] were investigated by this method. In these investigations the temperature dependence of the scattering was not studied. We carried out our measurements with a pure species of $tRNA^{Phe}$ (yeast) over a wide temperature range. Our preliminary results were communicated briefly elsewhere [5].

EXPERIMENTAL PROCEDURE

Materials

$tRNA^{Phe}$ (baker's yeast) was purified 42-fold from bulk tRNA from yeast (Boehringer Mannheim GmbH, Mannheim) by combination of extraction [6] and benzoyl-DEAE-cellulose chromatography [7]. It was chargeable to 82% when tested as described [8] and no foreign activity was found in the test by Neuhoff *et al.* [9]. The $tRNA^{Phe}$ (yeast) contained about 35% of intact 3'-end, the remainder was lacking the terminal adenylate, as indicated by alkaline hydrolysis and analysis of the resulting nucleosides. Before use the bulk tRNA and the $tRNA^{Phe}$ (yeast) were treated in the following way: (a) dialysis against 10 mM EDTA in twice distilled water; (b) dialysis two times against twice distilled water; (c) dialysis against 100 mM K_2SO_4 and 10 mM $MgSO_4$ in twice distilled water; (d) dialysis three times against twice distilled water; (e) lyophilisation; (f) solution in 0.05 M Tris-buffer at pH 7.5.

Methods

The X-ray small angle scattering measurements were carried out with Cu-K radiation. The small angle camera was a model developed in the Graz institute which is practically free from parasitic scattering [10]; a mechanically programmed step scanning device [11] allowed automatic operation. The solutions were investigated in Mark-capillaries of 0.1 cm diameter. The scattered Cu-K radiation was registered with a proportional counter and pulse height discriminator; the elimination of the K_β-line was carried out by a numerical method [12] developed in the Graz institute. A slit-shaped primary beam was used; the experimental curve therefore includes a collimation effect. This is indicated in the figures by a tilde (*e. g.* $\tilde{I}$, $\tilde{R}$). The collimation effect was elimi-

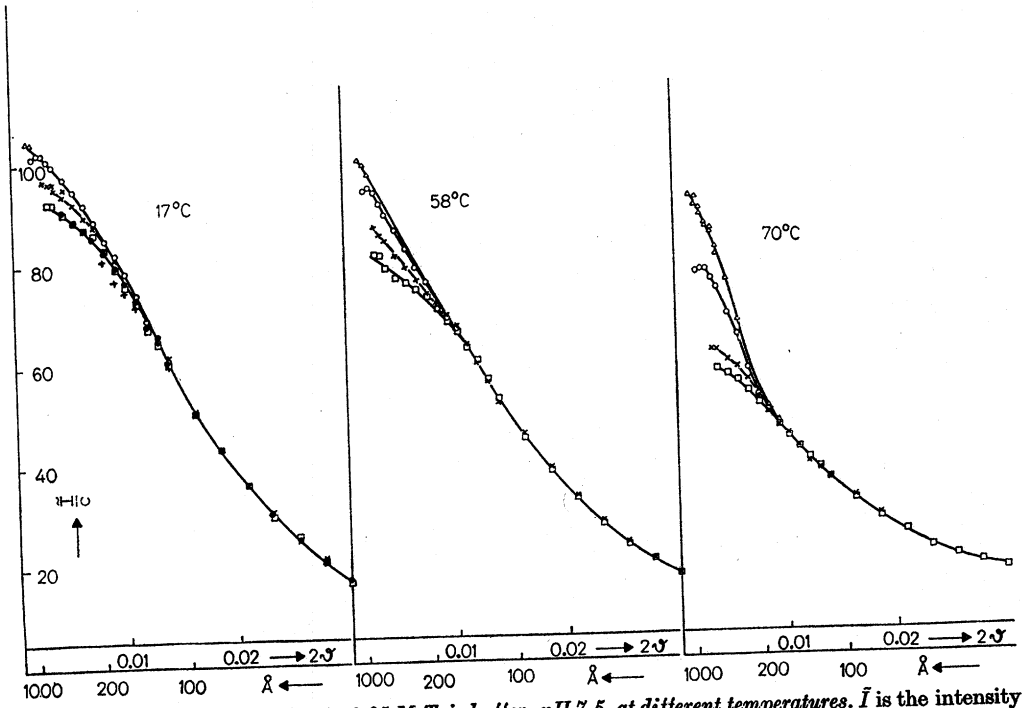

Fig. 1. *Scattering curves of tRNA^{Phe} (yeast) in 0.05 M Tris-buffer, pH 7.5, at different temperatures.* $\bar{I}$ is the intensity in imp./sec, c the concentration in mg/ml, the scattering angle 2ϑ is given in radians and the corresponding Bragg spacing in Å. The concentrations of the solution were 1.5 mg/ml (△), 3.03 mg/ml (○), 5.88 mg/ml (×), 10.6 mg/ml (●), 11.3 mg/ml (□) and 20.9 mg/ml (+)

nated according to the method of Guinier and Fournet [13] with the help of a computer program written in the Graz institute [14,15].

The measurements were extended to the smallest angle of 0.0015 radians, which corresponds to a Bragg's spacing of 1100 Å and to a largest angle of 0.14 radians. For the calculation of the molecular weight it is necessary to know the ratio of the scattered intensity at zero angle I_o to the intensity of the primary beam P_o. This quantity, called "absolute intensity", was determined with the help of a standard sample developed [17] and calibrated [16] in the Graz institute.

In order to measure the inner portions of the scattering curves concentrations of 1.5, 2, 3, 5 and 10 mg/ml were used. Since at larger angles even at higher concentrations no interparticular interference effects were observed, concentrations of 20, 30, 40 and 70 mg/ml were applied. All scattering curves were normalized for concentration, *i. e.*, the I/c values were always plotted (c concentration mg/ml; I intensity pulses/sec).

RESULTS

SIZE AND SHAPE OF tRNA^{Phe} (YEAST) AT 17°

Radius of Gyration

In Fig. 1 the inner portion of the experimental scattering curve is shown at different concentrations. The scattering curves have a Gaussian shape at small angles. A straight line is obtained, when plotting the logarithms of the scattered intensity, $\log I$, *versus* the square of the scattering angle $(2\vartheta)^2$ (Guinier plot) as shown in Fig. 2. At higher concentrations the scattered intensity in the inner portion is significantly lowered by interference effects. It can be eliminated in the manner indicated in Fig. 2 in the total scattering curve (compare [19]). Practically the same values for $\tilde{R}$ are found by the plot of Fig. 3.

After elimination of the collimation effect, the slope $\mathrm{tg}\,\alpha$ in the Guinier plot according to the formula [18]

$$R = \sqrt{3 \times 2.3 \times \mathrm{tg}\,\alpha}\ \frac{\lambda}{2\pi}\ \text{Å} \qquad (1)$$

gives the correct radius of gyration R of the macromolecule. It was determined to be 24.4 (±0.3) Å (Fig. 4, curve 1). Additional 10 mM Mg^{++} in the solution did not cause a significant change in the scattering curves. Such a change could have been expected from the hyperchromicity and crystallisation experiments. The radius of gyration in this case was 25.1 (±0.4) Å (Fig. 4, curve 2).

For comparison the scattering curve of bulk tRNA from yeast is given in Fig. 4, measured at 22°. A deviation from the straight line in the Guinier plot in the inner portion is obvious. This indicates that the solution is not completely homodisperse. That is,

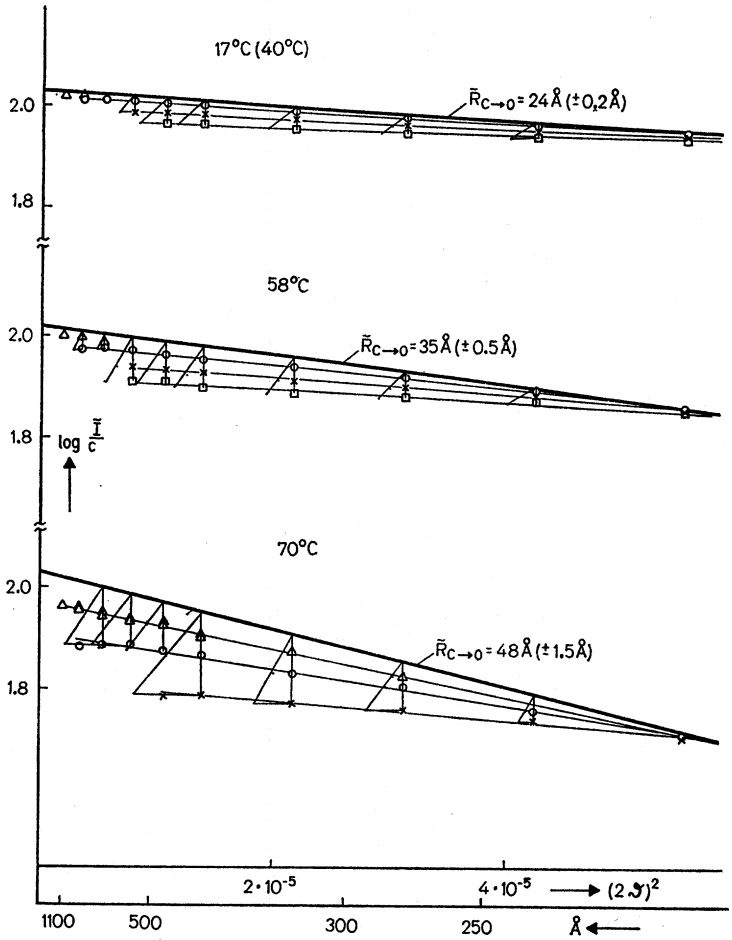

Fig. 2. *Guinier plot of the inner portion of the scattering curves in Fig. 1.* The concentrations of the solutions are the same as in Fig. 1. The strong lines correspond to the scattering curves extrapolated to zero concentration. The radii of gyration are given. The curves and the $\tilde{R}$-values are not corrected for the collimation-effect

besides the compact tRNA molecules some molecules are present as associated species or in unfolded forms.

Molecular Weight and Volume

In order to calculate the molecular weight M, the absolute scattering intensity I_o/P_o was determined as described in *Methods*. From the long straight course of the scattering curve in the Guinier plot (Fig. 4) an extrapolation to the value of the scattered intensity at zero angle I_o can be done quite unambiguously. From this value and the value of the partial specific volume $\bar{v}_1$ (0.54), we can calculate a molecular weight of 26100 from the following equation [20, 21, 1].

$$M = \frac{I_o/c}{P_o \times F} \quad \frac{a^2 \times 10^3}{D\,(z_1 - \bar{v}_1 \times \varrho_2)^2} \quad \frac{1}{i_o \times N_A}. \qquad (2)$$

In this equation F is the area of the counting tube slit in cm², c is the concentration of the dissolved substance in mg/ml, a the distance from the sample to the registering plane, D the thickness of the sample in cm, z_1 the number of electrons per gram of the dissolved substance; ϱ_2 the electron density of the solvent; i_o is the Thomson's constant (*i. e.* the scattering of the electron) and N_A Avogadro's number. The partial specific volume of $tRNA^{Phe}$ (yeast) was determined with a method recently developed in the Graz institute [22]. According to Porod the volume V of the particles in solution can be calculated from the invariant Q [23] of the scattering curve

$$Q = \int_0^\infty I \times (2\vartheta)^2 \times d\,(2\vartheta) \qquad (3)$$

and the scattered intensity I_o, by using (4)

$$V = \frac{I_o}{Q} \times \frac{\lambda^3}{4\pi}. \qquad (4)$$

We find $V = 41500\ (\pm 1200)$ Å³.

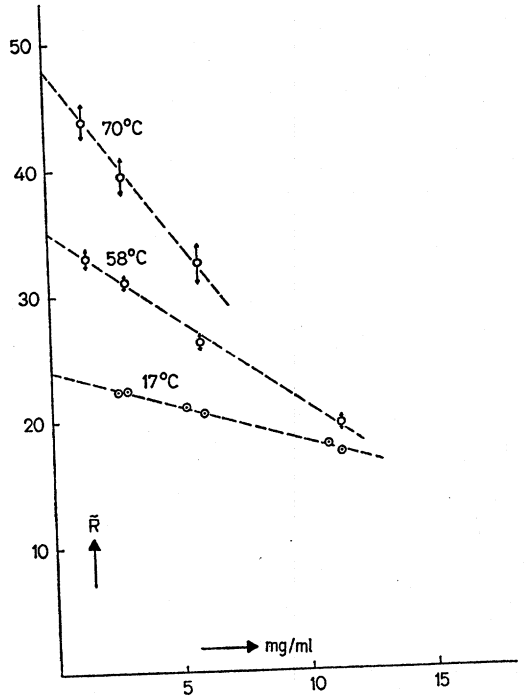

Fig. 3. *Radii of gyration* $\bar{R}$, *depending on concentration and temperature*

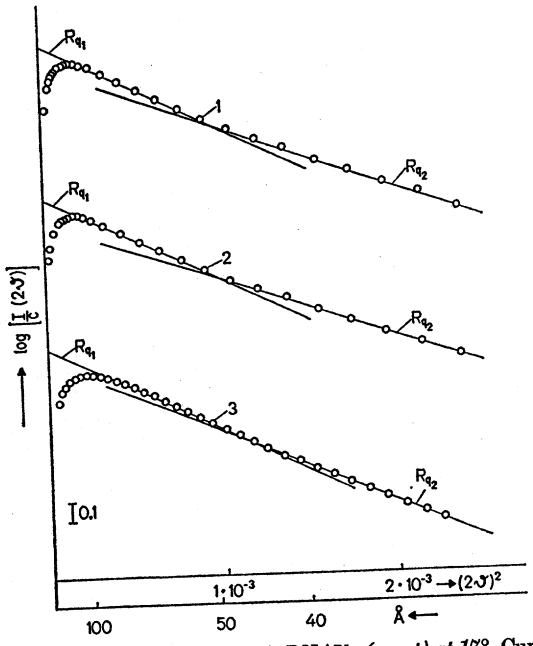

Fig. 5. *Cross-section factors of tRNA^{Phe} (yeast) at 17°.* Curve 1: in 0.05 M Tris-buffer and 10 mM Mg^{++}. $R_{q_1} = 11.0$ Å, $R_{q_2} = 9.5$ Å. Curve 2: in 0.05 M Tris-buffer $R_{q_1} = 11.0$ Å, $R_{q_2} = 9.1$ Å. Curve 3: cross-sectional curve of the model in Fig. 7. $R_{q_1} = 10.9$ Å, $R_{q_2} = 9.3$ Å

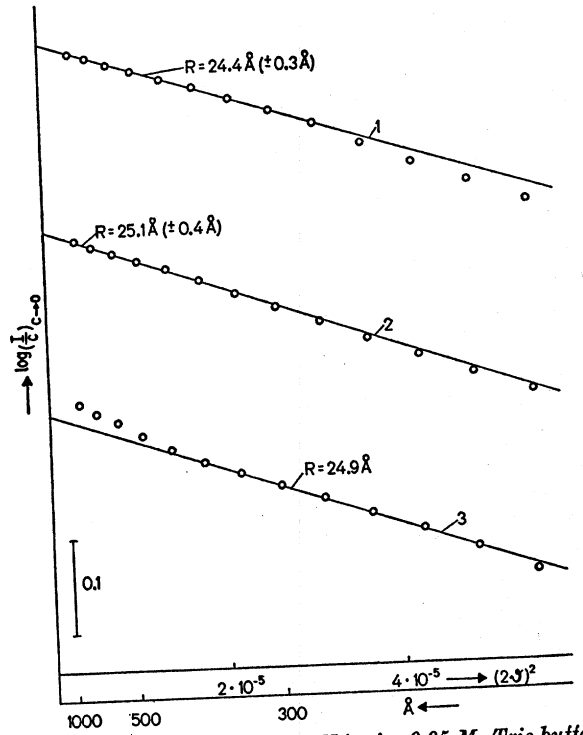

Fig. 4. *Scattering curves of tRNAs in 0.05 M Tris-buffer, extrapolated to zero concentration and after elimination of the collimation-effect.* Curve 1: tRNA^{Phe} (yeast) at 17°; curve 2: tRNA^{Phe} (yeast) at 17° and 10 mM Mg^{++}; curve 3: bulk tRNA from yeast at 22°

From the molecular weight M and the partial specific volume $\bar{v}$ the volume of the unswollen particle results directly. The comparison with the value obtained according to (4) gives the degree of swelling q:

$$q = \frac{N_A}{\bar{v}_1 \times 10^{24}} \times \frac{V}{M} = 1.77 \,. \qquad (5)$$

This value corresponds to 0.42 g H_2O per 1 g tRNA^{Phe} (yeast).

Cross-Section and Length of the Molecule

The scattering curve of an elongated particle can be presented as the product of a Lorentz factor (proportional to $1/2\vartheta$) and a cross-sectional factor of the Gaussian type [24]. By multiplying by the scattering angle 2ϑ, the Lorentz-factor is eliminated. From the cross-sectional factor obtained in this way, conclusions can be drawn on the cross-section of the molecule provided that the ratio of length to diameter is larger than 1.5 (*i. e.* $R/R_q > 1.5$) [25]. In Fig. 5 the cross-sectional curves of tRNA^{Phe} (yeast) are plotted as measured with and without 10 mM Mg^{++}. They are almost identical.

From the Guinier plot of the cross-sectional factor $\log (I \times 2\vartheta)$ *versus* $(2\vartheta)^2$, the radius of gyration of the cross-section R_q may be determined in analogy to (1):

$$R_q = \sqrt{2 \times 2.3 \times \operatorname{tg}\alpha} \times \frac{\lambda}{2\pi} \text{ Å} \qquad (6)$$

R_q was found to be 11.0 Å (in systems containing different cross-sections this value represents a mean radius of gyration).

If R and R_q are known, the length of the particle may be calculated from equation (7), assuming a cylindrical shape.

$$R^2 - R_q^2 = L^2/12 \,. \tag{7}$$

Thus we obtain the value of 75 Å for the length L of the particle. (Assuming an ellipsoid we obtain with the same radii of gyration R and R_q a maximum length of 97 Å).

There is another way to calculate the length of a particle that is from the molecular weight M and the mass per 1 Å length ($M/1$ Å) of the particle. In analogy to (2) the absolute intensity of the cross-sectional factor can be used to calculate the mass per 1 Å length [24,1,20] of the particle using (8)

$$M/1\,\text{Å} = \frac{(I/c \times 2\vartheta)_o}{P_o \times F} \times \frac{a^2 \times 10^3}{D\,(z_1 - \bar{v}_1 \times \varrho_2)^2} \times \frac{2}{i_o \times N_A} \tag{8}$$

$M/1$ Å was found to be 344.

By dividing M (26100) by $M/1$ Å (344) a value of 76 Å is obtained for the length. Since this value is in good agreement with the value calculated from the radii of gyration, the shape of the tRNA^{Phe} (yeast) molecule is approximated well by a cylindrical body which has a length of 75—76 Å.

Determination of the Shape

The comparison of the experimental scattering curve (Fig. 6) with the calculated curves [26] of triaxial bodies, led to a ratio of diameter to length of about 1:2.5 (Fig. 7), assuming rotational cylinders.

A more detailed determination of the shape shows that the tRNA^{Phe} (yeast) molecule cannot be interpreted by a cylinder of an uniform cross-section. The experimental scattering curves differ clearly from the theoretical curves of simple cylinders; in particular the curves of the cross-section show in the Guinier plot two different regions. The inner, steeper portion yields a R_{q1}-value of 11.0 Å, while the outer, flatter portion yields R_{q2}-values in the range of 9.5 Å to 9.1 Å as shown in Fig. 5.

This indicates that there are two portions of the molecule with different cross-sections; therefore we calculated the scattering curves for a number of different models. Due to the limitations of computer programs available, only ellipsoids instead of cylinders could be used. This substitution however should not substantially affect the results. A calculation with cylinders is in preparation.

The best agreement with the experimental curve is given by the model shown in Fig. 7. It consists of 3 ellipsoids with their main axes arranged parallel. The axes of the large ellipsoid have the following

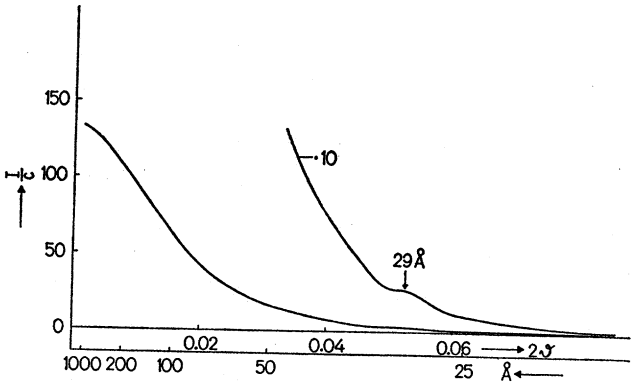

Fig. 6. *Scattering curve of tRNA^{Phe} (yeast) at 17°*

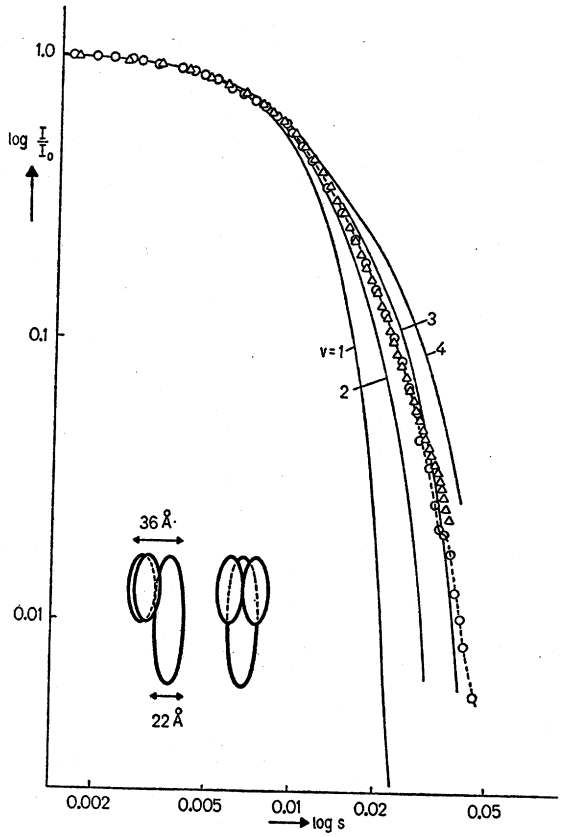

Fig. 7. *Experimental scattering curve (○) of tRNA^{Phe} (yeast) at 17° compared with the theoretical scattering curves of rotational cylinders of various axial ratios* ν *(closed lines) and with the theoretical curve of the model formed from three ellipsoids (△) in log — log plot.* $s = 2 \sin \vartheta/\lambda$

dimensions (in Å): $a = 11$, $b = 11$, $c = 46$, and the two small ellipsoids have dimensions of $a = 9$, $b = 9$, $c = 24$. The radius of gyration and the volume of this model is in good agreement with the experimental values. Assuming the same radius of gyration the long axes of ellipsoids are longer than the correspond-

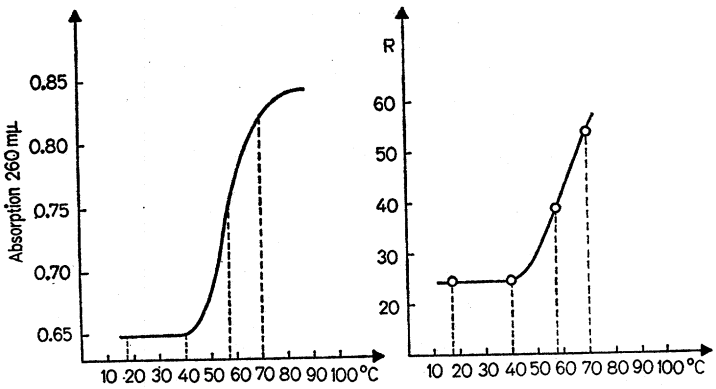

Fig. 8. *Melting curve of tRNA^{Phe} (yeast) and dependence of the radius of gyration on the temperature*

Table. *Measurements on tRNA^{Phe} (yeast) in 0.05 M Tris-buffer, pH 7.5*

Temp.	Mg^{++}	R	M	V	q
°C	mM	Å		Å³	g H_2O/g tRNA
17	—	24.4 (±0.3)	26100	41500 (±1200)	0.42
17	10	25.1 (±0.4)	26300		
40	—	24.4 (±0.3)	26100		
58	—	39 (±1)	26000		
70	—	54 (±2)	26000		

ing lengths of cylinders. The scattering curve of the model is in agreement with the experimental curve (Fig. 7).

The cross-sectional curve of the model is nearly identical to the experimental curves (Fig. 5). The calculation for the model shows two different regions in the Guinier plot with values $R_{q1} = 10.9$ Å and $R_{q2} = 9.3$ Å in good agreement with the experimental values.

The model in Fig. 7 has two different cross-sections, with diameters of 20—22 Å and 36 Å, respectively.

CHANGE OF CONFORMATION OF tRNA^{Phe} (YEAST) ON INCREASING TEMPERATURE

It is not possible to obtain exact information on the actual shape of the molecule by the method of X-ray small angle scattering, but the method is highly sensitive with respect to changes of conformation of a molecule. We therefore studied the conformational change of tRNA, which accompanies the melting of base pairs. In Fig. 8 the optical-melting curve of the tRNA^{Phe} (yeast) in 0.4 M phosphate buffer at pH 7.0 is given. The T_m-value lies at 57°.

The small angle scattering measurements were done at 17°, 40°, 58° and 70° in 0.05 M Tris buffer at pH 7.5 (Table). At each temperature several concentrations were measured.

Measurements at 40°

On increasing the temperature from 17° to 40° no significant change of the scattering curve of tRNA^{Phe} (yeast) was observed as shown in Fig. 9 (curve 3). This is in good agreement with the melting-curve, given in Fig. 8. For comparison the scattering curve of bulk tRNA from yeast at 22° (curve 1) and at 40° (curve 2) is given in Fig. 9. It can be seen immediately, that the tRNA-mixture shows a considerable change of the scattering curve, which is reversible. Apparently some of the molecules have already lost their tertiary structure or begun to unfold. This result is in agreement with studies on hyperchromicity of tRNA. For instance tRNA^{Ser} (yeast) begins to melt at 30°. Therefore it seems impossible to obtain quantitative data from a mixture in which some of the molecules are still compact and unmelted (*e. g.* tRNA^{Phe}) and the rest of the molecules are already partly unfolded. For this reason measurements at higher temperatures were only carried out with tRNA^{Phe} (yeast).

Curves 1 and 2 in Fig. 9 indicate that a change of conformation of tRNA mixture can only be observed if the measurements are extended to fairly small angles corresponding to a Bragg spacing of at least 1000 Å. If the scattering intensity is recorded only up to a Bragg spacing of 300 Å, only a slight rise of the radius of gyration and a strong decrease of the absolute intensity are observed. This could be misunderstood as a decomposition of some of the molecules.

Measurements at 58° and 70°

If solutions of tRNA^{Phe} (yeast) are exposed too long to high temperature and X-ray radiation, irreversible changes in the tRNA molecules may occur. To make sure that there are no changes during the measurements, the following technique was applied. In each measurement first a few points of the scattering curves at 17° were registered. After that the solution was brought to the desired temperature

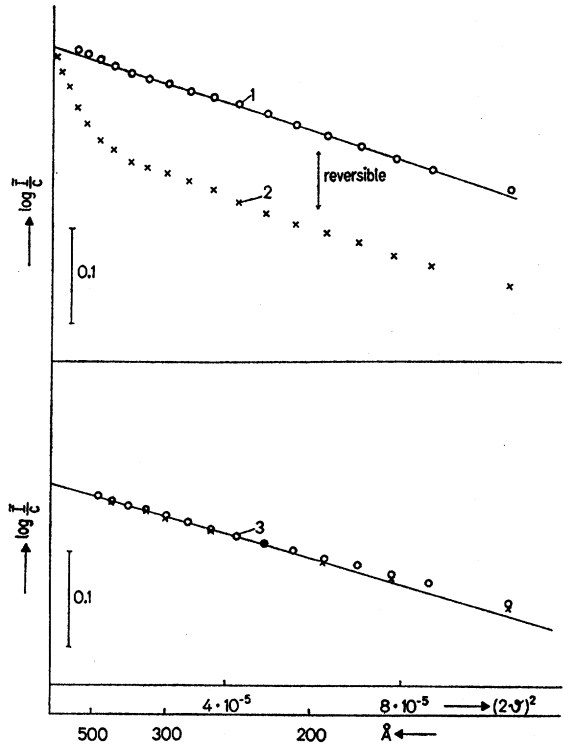

Fig. 9. *Scattering curves in Guinier-plot.* Curve 1: bulk tRNA at 22°; curve 2: bulk tRNA at 40°; curve 3: $tRNA^{Phe}$ (yeast) at 17° (○) and at 40° (×)

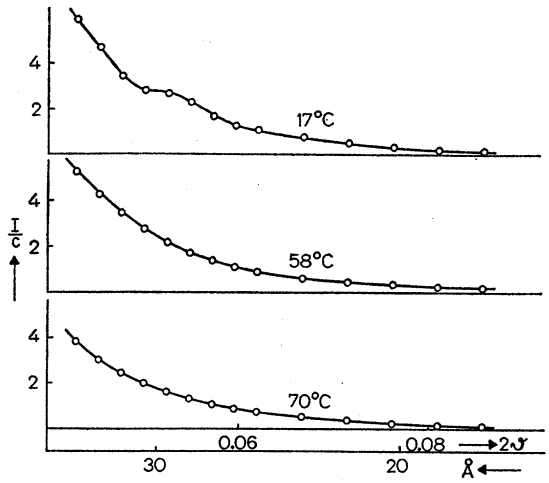

Fig. 10. *Outer portion of the scattering curve of $tRNA^{Phe}$ (yeast)*

(58° or 70°) and the scattering curve was measured for 1 or 2 hours. Then the solution was cooled again to 17° and the intensity values measured first were checked. If the measurements at high temperature were carried out within 1 to 3 hours, a complete reversibility of the conformational changes was observed. In Fig. 1 the inner portions of the experimental scattering curves at different temperatures are shown. Fig. 2 and 3 demonstrate the extrapolation to zero concentration, as described above. These figures indicate that the radius of gyration strongly increases with increasing temperature. Also, strong interference effects are observed at higher temperatures. Therefore we had to work with highly dilute solutions. The measurements at 58° and 70° could therefore not be performed with the same degree of precision as the measurements at 17°. This is seen in Fig. 2 and Fig. 3.

In Fig. 8 the radii of gyration (after elimination of the collimation effect) are plotted *versus* the temperature, and the melting curve of $tRNA^{Phe}$ (yeast) is shown. Both curves exhibit similar shapes. The change in conformation at the melting temperature goes parallel with an expansion of the molecule.

The cross-sectional curves also indicate that at high temperatures somewhat different cross-sections are present. A quantitative interpretation of these curves was not possible, but a significant decrease of the average R_q with increasing temperature could be observed, *i. e.*, smaller cross-sections appear.

In Fig. 10 the outer portions of the scattering curves are given. At 17° the scattering curve exhibits clearly a submaximum at a Bragg spacing of 29 Å. This can also be seen in Fig. 6. On increasing the temperature to 58° and 70° this shoulder disappears. After cooling down to 17°, the shoulder appears again. This shoulder apparently is due to the conformation of the compact $tRNA^{Phe}$ (yeast) and is lost on unfolding.

Random Coil Conformation at 70°

The scattering curve of the $tRNA^{Phe}$ (yeast) at 70° has a course typical for relatively short chains. The scattering curve of a coiled molecule in solution is known to be composed of three portions [27—29]: the inner portion according to a Gaussian curve is due to the coil as a whole. The middle portion obeys a $1/(2\vartheta)^2$ law and the exterior a $1/2\vartheta$ law. The transition point between these two outer portions is most distinct if $I \times (2\vartheta)^2$ is plotted *versus* 2ϑ, as seen in Fig. 11. From the position of this transition point, one can draw conclusions on the average curvature of the chain, which is defined by the "persistence length". According to the equation

$$\bar{a} = 2 \times 2.3 \times \frac{\lambda}{4\pi} \times \frac{1}{(2\vartheta)^*} \qquad (9)$$

a persistence-length $\bar{a}$ of 30 Å can be calculated from the $(2\vartheta)^*$ abscissa-value of the transition point. For comparison a scattering curve calculated according to the Monte-Carlo method [30] with the same persistence length is also plotted. There the number x of the persistence lengths is chosen to be 18. $tRNA^{Phe}$

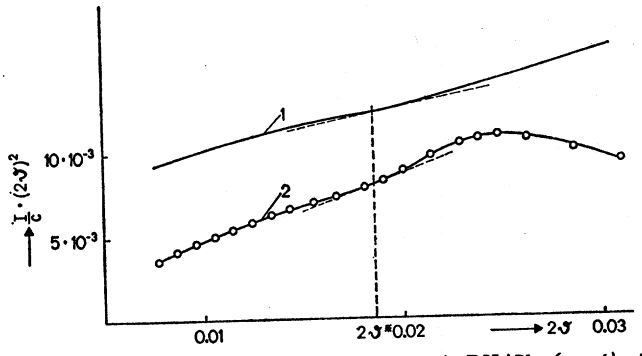

Fig. 11. *Experimental scattering curve of tRNA^{Phe} (yeast) at 70° (curve 2) and theoretical scattering curve of a coil calculated according to the Monte-Carlo method for 18 persistence length (curve 1)*

(yeast) consists of 75 nucleotides, each being 7.2 Å long. The molecule therefore must have a length L of 540 Å, if it is maximally stretched in one direction. The number x of the persistence lengths, necessary for the calculation of the theoretical curve, is obtained by dividing L by $\bar{a}$.

The agreement between the experimental and theoretical curve is satisfactory. The slope of the experimental curve at larger angles is due to the influence of the finite cross-section as shown by Kirste [31]. From these studies it can be concluded that the unfolding of tRNA^{Phe} (yeast) molecule has advanced at 70° so far that it has a coil-conformation.

The Influence of Magnesium

In the presence of 10 mM Mg^{++} at high temperatures, only preliminary measurements were done.

At 58° a modest and at 70° a strong increase of the radius of gyration was observed. These curves were similar to the scattering curves of tRNA^{Phe} (yeast), which were obtained in absence of Mg^{++} at 58°. This rather qualitative result is again in good agreement with the hyperchromicity measurements, which show that in the presence of 10 mM Mg^{++} the melting begins at higher temperatures and that under these conditions the melting point of tRNA^{Phe} (yeast) lies at 73°. (In a Mg^{++} free buffer the melting point is at 57°.)

DISCUSSION

Our experiments are done with a highly purified single species of tRNA, tRNA^{Phe} (yeast). This seems to be necessary in order to obtain definite data from X-ray small angle scattering. In a mixture of tRNAs as shown in Fig. 9, the scattering curve is composed of several superimposed curves as observed in a mixture of polydispersed molecules. The conformational stability differs from tRNA to tRNA. Some of the tRNAs in a mixture might have a partly opened structure even at room temperature. tRNA^{Phe} (yeast) on the other hand is rather rigid as known from chemical and physical data [32,33]. There are also some tRNAs which tend to form dimeric particles easily, such as tRNA^{Ser} (yeast).

The observed radius of gyration $R = 24.4$ Å for tRNA^{Phe} (yeast) at room temperature is close to the values obtained by Lake and Beeman [2] ($R = 23.5$ Å for bulk tRNA from yeast at 22.5°) and Krigbaum and Godwin [3] [$R = 23.9$ Å for bulk tRNA from yeast and $R = 23.2$ Å for tRNA^{Ala} (yeast)].

The fact that two different cross sections are observed, rules out a simple triaxial body for the molecule. Models like a symmetrical H-model [2] or almost symmetrical arrangements by folding all arms together [34] can be excluded, whereas others are compatible with the results [4,32,35].

The two different cross sections might be interpreted in the following way: the diameter of 22 Å corresponds to the diameter of a single Watson and Crick helix and can be attributed to the anticodon arm. The cross section of 36 Å diameter is in agreement with a compact part of the molecule where parts of the cloverleaf are folded together.

The cross sections of the model formed by folding together dihydrouridine loop, T-Ψ-C-G loop and C-C-A end [32] fit with the above data. Also the length/overall width ratio (2.5) is in agreement with that model. The overall radius of gyration (24.4 Å) is, however, larger than expected for the model. One should however take into consideration that a highly solvated poly-anion with an ionic layer around itself might show anomalies [36—38] which do not allow a direct correlation between measured and calculated R-values. A correction for the kind of ions and the sphere of hydration might be necessary [39].

The molecular weight as determined from the X-ray scattering is 26100, as compared to the value from the known sequence of 24890 (without counter ions). The volume (4.1×10^4 Å^3) of the particle in solution is in good agreement with the data obtained from X-ray diffraction work on single crystals [40]. From the size of the unit cell and the number of molecules in it, a volume per molecule of 3.84×10^4 Å^3 is calculated [40].

The temperature dependency of the scattering data can easily be explained by a transformation of the highly structured conformation of tRNA^{Phe} (yeast) into a random coil. This unfolding is also reflected in a strong increase in viscosity as determined by Henley *et al.* [41].

Note

After our paper having been presented for printing, the publication of Connors *et al.* [42] on X-ray small angle scattering of various tRNA species

nas appeared. We have compared our scattering curves with those of Connors *et al.* and Ninio *et al.* [4]. Our scattering curve agrees well with the curves of Connors *et al.*, only the low peak at a Bragg spacing of 29 Å is not present in the scattering curves of Connors *et al.* Also the radii of gyration ($R = 23.5-25$ Å) and the dimensions 25 by 35 by 85 Å named by the authors agree with our value ($R = 24.4$ and 25.1 Å) and the dimensions of our model composed of ellipsoids (diameters 22 and 36 Å, length 92 Å).

The scattering curve of Ninio *et al.*, however, deviates especially in the tail end from the scattering curves of Connors *et al.* and of ours; the radius of gyration of 25 Å corresponds to our value.

This research has been financed in part by a grant made by the United States Department of Agriculture under P. L. 480. This work was also supported by research grants from the Österreichische Forschungsrat. We (I. P. and O. K.) wish to thank Miss Müller for experimental help. We (F. C., F. v. d. H., and E. S.) are also grateful to Dr. K. Holmes, Dr. G. Schulz and Dr. W. Kapsch, Max-Planck-Institut für Medizinische Forschung, Heidelberg, and Dr. A. Maelicke and Dr. D. Gauß, Max-Planck-Institut für Experimentelle Medizin, Göttingen, for helpful discussion and criticism.

REFERENCES

1. Kratky, O., *Progr. Biophys.* 13 (1963) 105.
2. Lake, J. A., and Beeman, W. W., *J. Mol. Biol.* 31 (1968) 115.
3. Krigbaum, W. R., and Godwin, R. W., *Science*, 154 (1966) 423.
4. Ninio, J., Favre, A., and Yaniv, M., *Nature (London)*, 223 (1969) 1333.
5. Kratky, O., Pilz, I., Cramer, F., von der Haar, F., and Schlimme, E., *Monatsh. Chem.* 100 (1969) 748.
6a. Khym, J. X., *Biochemistry*, 2 (1963) 401.
6b. Khym, J. X., *J. Biol. Chem.* 240 (1965) Pc 1488.
7. Gillam, I., Millward, S., Blew, D., von Tigerstrom, M., Wimmer, E., and Tener, G. M., *Biochemistry*, 6 (1967) 3043.
8. Schlimme, E., von der Haar, F., and Cramer, F., *Z. Naturforsch.* 24b (1969) 631.
9. Neuhoff, V., von der Haar, F., Schlimme, E., and Weise, M., *Hoppe Seyler's Z. Physiol. Chem.* 350 (1969) 121.
10a. Kratky, O., *Z. Elektrochem.* 58 (1954) 49; 62 (1958) 66.
10b. Kratky, O., and Skala, Z., *ibid* 62 (1958) 73.
11a. Kratky, Ch., and Kratky, O., *Z. Instrumentenk.* 72 (1964) 302.
11b. Leopold, H., *Elektronik* 14 (1965) 359.
12. Zipper, P., *Acta Phys. Austriaca*, 30 (1969) 143.
13. Guinier, A., and Fournet, G., *J. Phys. Radium*, 8 (1947) 345.
14. Kratky, O., Porod, G., and Skala, Z., *Acta Phys. Austriaca*, 13 (1960) 76.
15. Heine, S., and Roppert, J., *Acta Phys. Austriaca*, 15 (1962) 148.
16. Kratky, O., and Wawra, H., *Monatsh. Chem.* 94 (1963) 981.
17a. Kratky, O., Pilz, I., and Schmitz, P. J., *J. Colloid Interface Sci.* 21 (1966) 24.
17b. Pilz, I., and Kratky, O., *ibid.* 24 (1967) 211.
17c. Pilz, I., *ibid.* 30 (1969) 140.
18. Guinier, A., and Fournet, G., *Small Angle Scattering of X-Rays*. Wiley, New York and Chapman & Hall, London 1955.
19. Cleemann, J. C., and Kratky, O., *Z. Naturforsch.* 15b (1960) 525.
20. Kratky, O., *Z. Anal. Chem.* 201 (1964) 161.
21. Kratky, O., Porod, G., and Kahovec, L., *Z. Elektrochem.* 55 (1951) 53.
22. Stabinger, H., Leopold, H., and Kratky, O., *Monatsh. Chem.* 98 (1967) 436; Kratky, O., Leopold, H., and Stabinger, H., *Z. Angew. Phys.* 27 (1969) 273.
23. Porod, G., *Kolloid-Z.* 124 (1951) 83.
24a. Kratky, O., and Porod, G., *Acta Phys. Austriaca*, 2 (1948) 133.
24b. Porod, G., *ibid.* 2 (1948) 255.
24c. Kratky, O., and Porod, G., In *Die Physik der Hochpolymeren* (herausgegeben von H. A. Stuart). Springer-Verlag, Berlin-Göttingen-Heidelberg 1953, Band 2, p. 515.
25. Mittelbach, P., *Acta Phys. Austriaca*, 19 (1964) 53.
26. Mittelbach, P., and Porod, G., *Acta Phys. Austriaca*, 14 (1961) 185; 14 (1961) 405; 15 (1962) 122.
27. Heine, S., Kratky, O., Porod, G., and Schmitz, P. J., *Makromol. Chem.* 44—46 (1961) 682.
28. Kratky, O., and Porod, G., *Rec. Trav. Chim. Pays-Bas*, 68 (1949) 1106.
29. Porod, G., *J. Polymer Sci.* 10 (1953) 157.
30. Heine, S., Kratky, O., and Roppert, J., *Makromol. Chem.* 56 (1962) 150.
31. Kirste, R. G., *Z. Physik. Chem., Neue Folge*, 36 (1968) 265.
32. Cramer, F., Doepner, H., von der Haar, F., Schlimme, E., and Seidel, H., *Proc. Nat. Acad. Sci. U. S. A.* 61 (1968) 1384.
33a. Litt, M., *Biochemistry*, 8 (1969) 3249.
33b. Nishimura, S., personal communication.
34. Melcher, G., *FEBS Letters*, 3 (1969) 185.
35. Levitt, M., *Nature (London)*, 224 (1969) 759.
36. Luzzati, V., Nicolaieff, A., and Masson, F., *J. Mol. Biol.* 3 (1961) 185.
37. Timasheff, S. N., Witz, J., and Luzzati, V., *Biophys. J.* 1 (1961) 525.
38. Rolfe, R., and Meselson, M., *Proc. Nat. Acad. Sci. U.S.A.* 45 (1959) 1039.
39. Kirste, R. G., and Stuhrmann, B. H., *Z. Physik. Chem., Neue Folge*, 56 (1967) 5/6.
40. Cramer, F., von der Haar, F., Holmes, K. C., Saenger, W., Schlimme, E., and Schulz, G. E., *J. Mol. Biol.*, in press.
41. Henley, D. D., Lindahl, T., and Fresco, J. R., *Proc. Nat. Acad. Sci. U. S. A.* 55 (1966) 191.
42. Connors, P. G., Labanauskas, M., and Beeman, W. W., *Science*, 166 (1969) 1528.

I. Pilz and O. Kratky
Institut für Physikalische Chemie der Universität
Heinrichstraße 28, A-8010 Graz, Austria

F. Cramer, F. von der Haar, and E. Schlimme
Max-Planck-Institut für Experimentelle Medizin
Abteilung Chemie
BRD-3400 Göttingen, Hermann Rein-Straße 3, Germany